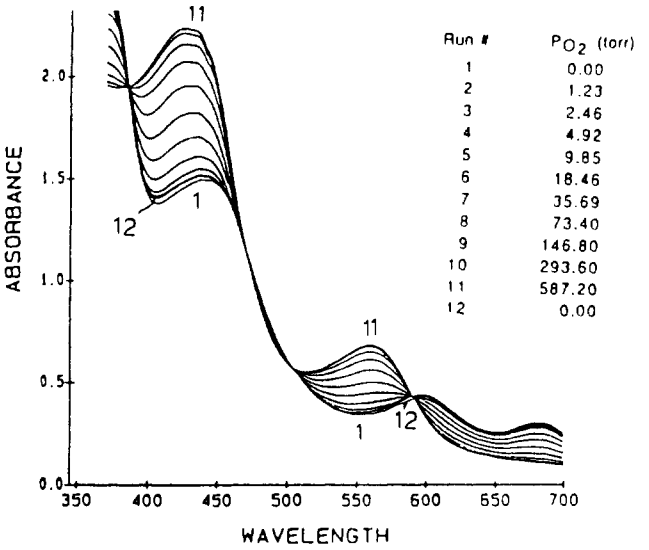

Figure 7. Dioxygen spectral titration for [Co(Me$_4$(C$_6$F$_5$CO)$_2$bz$_2$hexaenatoN$_4$)] at 258 K in toluene/pyridine solution.

Figure 7 presents the spectra obtained at various partial pressures of O_2 at −15 °C for the perfluorobenzoyl derivative. The spectra have clean isosbestic points at 385 and 590 nm. Purging with N_2 for 20 min reverses the oxygenation process almost completely.

The decomposition of the perfluorobenzoyl complex was monitored at −5 and 15 °C for 10^{-3} M toluene solutions containing 100-fold excess of pyridine. The complex was fully oxygenated, and the decay of the bands at 425 and 555 nm was monitored. The half-life for decay is about 10 h at 5 °C, but the decomposition rate was not the same for the two wavelengths. The decay only approximates a simple exponential function and is therefore not a simple first-order process. At 15 °C, the complex decomposes with a half-life of at least 2 h, and the wavelength dependence is more pronounced. These preliminary observations indicate that these new oxygen carriers are subject to irreversible autoxidation processes. In this way they are comparable to most other dioxygen carriers. Further, the decomposition process appears to be complicated, but its nature could only be revealed by more detailed studies.

Electrochemical Behavior of the Macrocyclic Cobalt Complexes. The cobalt couples are quasi reversible with $(E_p^C - E_p^A)/2$ values that are less than 120 mV. This strongly supports the view that the autoxidation processes do not involve ligand oxidation, a result of considerable importance. For many purposes, the ability of the oxygen carrier to function can be restored by the addition of reducing agents, so long as the ligand is not oxidized.

The benzoyl complex is the most cathodic and thus should exhibit the highest dioxygen affinity,[25] as has indeed been observed. The trend is as expected for the trifluoroacetyl and the perfluorobenzoyl complexes.

Acknowledgment. The financial support of Air Products and Chemicals, Inc., is gratefully acknowledged. Dr. David Chan and C. Weisenberger of the Department provided the mass spectral measurements, and Carl Engelman of the Department helped in the NMR studies. These contributions are deeply appreciated.

(25) Carter, M. J.; Rillema, D. P.; Basolo, F. *J. Am. Chem. Soc.* **1974**, *96*, 392.

Contribution from the Laboratoire de Synthèse et d'Electrosynthèse Organométallique Associé au CNRS (UA 33), Faculté des Sciences "Gabriel", Université de Bourgogne, 6 Boulevard Gabriel, 21100 Dijon, France, and Department of Chemistry, University of Houston, Houston, Texas 77204-5641

Disulfur and Diselenium Titanium(IV) Porphyrins: Synthesis and Characterization of (P)Ti(η^2-S$_2$) and (P)Ti(η^2-Se$_2$), Where P is One of Several Different Porphyrin Rings. Crystal Structure of (5,10,15,20-Tetra-*p*-tolylporphinato)perthiotitanium(IV)

R. Guilard,*[1a] C. Ratti,[1a,b] A. Tabard,[1a] P. Richard,[1a] D. Dubois,[1b] and K. M. Kadish*[1b]

Received August 8, 1989

The synthesis and characterization of various disulfur and diselenium titanium(IV) porphyrins are presented. Each compound was synthesized by one of two methods. The first involves an oxidative addition of Cp_2TiS_5 or Cp_2TiSe_5 to (P)TiF under an inert atmosphere and leads to the corresponding (P)Ti(η^2-S$_2$) or (P)Ti(η^2-Se$_2$) derivative, where P is the dianion of octaethylporphyrin (OEP), tetraphenylporphyrin (TPP), tetra-*p*-tolylporphyrin (TpTP), tetra-*m*-tolylporphyrin (TmTP), tetramesitylporphyrin (TMP), or tetrakis(*p*-(trifluoromethyl)phenyl)porphyrin (TpCF$_3$PP). The same series of complexes was also obtained by a substitution reaction involving (P)TiF$_2$ and either Cp_2TiS_5 or Cp_2TiSe_5. Each disulfur and diselenium compound was characterized by mass spectrometry and IR, UV-visible, and ^{1}H NMR spectroscopies as well as by electrochemistry. The crystal structure of (TpTP)Ti(η^2-S$_2$) was determined by X-ray diffraction (monoclinic, $P2_1/n$, a = 14.688 (2) Å, b = 14.822 (2) Å, c = 19.308 (4) Å, β = 90.51 (2)°, Z = 4, $R(F_o)$ = 0.047, $R_w(F_o)$ = 0.0494). The S$_2$ entity is "side-on" bonded to the titanium atom. The S–S bond length is 2.042 (2) Å, the two Ti–S bond lengths are 2.283 (2) and 2.311 (2) Å, and the mean Ti–N bond length is 2.10 (2) Å.

Introduction

Numerous organometallic compounds containing transition-metal–chalcogen bonds have been characterized.[2] Chalcogen atoms may bind metals in a large variety of bridging geometries or they may act as terminal ligands.[2,3] Metalloporphyrins containing oxo or peroxo axial ligands have been well characterized,[4-20] but little data[21-25] are available for porphyrins with sulfur or

(1) (a) Université de Bourgogne. (b) University of Houston.
(2) Draganjac, M.; Rauchfuss, T. B. *Angew. Chem., Int. Ed. Engl.* **1985**, *24*, 742.
(3) Müller, A.; Jaegermann, W.; Enemark, J. H. *Coord. Chem. Rev.* **1982**, *46*, 245.
(4) Guilard, R.; Lecomte, C. *Coord. Chem. Rev.* **1985**, *65*, 87.
(5) Matsuda, Y.; Murakami, Y. *Coord. Chem. Rev.* **1988**, *92*, 157.
(6) Boucher, L. J. *Coord. Chem. Rev.* **1972**, *7*, 289.
(7) Cheung, S. K.; Grimes, C. J.; Wong, J.; Reed, C. A. *J. Am. Chem. Soc.* **1976**, *98*, 5028.
(8) James, B. R. In *The Porphyrins*; Dolphin, D., Ed.; Academic: New York, 1978; Vol. V, Chapter 6.
(9) Dolphin, D.; James, B. R.; Welborn, H. C. *Adv. Chem. Ser.* **1982**, *No. 201*, 563.

0020-1669/90/1329-2532$02.50/0

selenium axially bonded ligands. An oxo type ligation of the chalcogen atom occurs in (P)VS and (P)VSe, where P is the dianion of octaethylporphyrin, tetraphenylporphyrin, tetra-*p*-tolylporphyrin, and tetra-*m*-tolylporphyrin.[25] The coordination of thiolate ligands by Ti(III) and Ti(IV) porphyrins is also known,[21] but until recently, titanium porphyrins coordinated with Se ligands had not been synthesized.

In a preliminary communication,[26] we reported a method for preparing (P)Ti(η^2-S_2) and (P)Ti(η^2-Se_2) from (P)TiF[27] and also presented an X-ray structure of (TpTP)Ti(η^2-S_2). These compounds provided the first examples in porphyrin chemistry for a M(η^2-Y_2) moiety where Y = S or Se. This present paper expands upon the initial communication[26] and reports two synthetic routes to obtain titanium(IV) perthio and perseleno metalloporphyrins. These compounds were characterized by mass spectrometry and IR, UV-visible, and ^{1}H NMR spectroscopies as well as by electrochemistry and suggest the presence of a cis-coordinated S_2^{2-} or Se_2^{2-} unit in (P)Ti(η^2-S_2) and (P)Ti(η^2-Se_2).

The data in this study should lead to a better understanding of porphyrin metal–chalcogen bonds in porphyrins. Peroxo ligand complexes of Ti(IV) porphyrins are well-known,[17,18,28,29] and the data from this present study should also enable comparisons to be made between the structural properties and reactivity of peroxo, perthio, and perseleno porphyrin derivatives of the form (P)Ti(η^2-Y_2), where Y = O, S, or Se.

Experimental Section

Chemicals. All solvents were thoroughly dried in an appropriate manner and distilled under argon prior to use. (P)TiO,[30] (P)TiF_2,[31] and (P)TiF,[32,33] where P = TPP, TmTP, TpTP, $TpCF_3PP$, TMP, or OEP were synthesized by literature methods. Tetra-*n*-butylammonium perchlorate (TBAP) was purchased from Eastman Kodak Co., twice recrystallized from absolute ethyl alcohol, and dried in a vacuum oven at 40 °C prior to use.

Synthesis of (P)Ti(η^2-S_2) and (P)Ti(η^2-Se_2). Two different methods were utilized for preparation of the chalcogen complexes. These are labeled as method A and method B and are described below.

Method A. A suspension of (P)TiF_2 (0.66 mmol) in toluene (180 cm^3) was reduced by zinc amalgam (1 g) and refluxed for 6 h to give a pink solution of (P)TiF. Cp_2TiS_5 or Cp_2TiSe_5 (1.48 mmol) was then added to the mixture, which was heated under reflux for 8 h. The solvent was evaporated under reduced pressure, and the crude product chromatographed on a silica column using toluene as eluent. The resulting dark red solution was evaporated to dryness and the solid residue recrystallized from toluene or heptane, giving yields between 61 and 88%.

Method B. Cp_2TiS_5 or Cp_2TiSe_5 (0.87 mmol) was mixed with (P)TiF_2 (0.66 mmol) in toluene (140 cm^3). The mixture was refluxed for 12 h, after which the solvent was evaporated and the residual solid purified as described above. Recrystallization was carried out from a toluene/heptane mixture and gave yields similar to those obtained according to the method A.

Physical and Electrochemical Measurements. Elemental analyses were performed by the "Service de Microanalyse du CNRS". Mass spectra were recorded by the "Centre de Spectrométrie de Masse du CNRS" in the electron-impact mode with a VG 70-70 spectrometer (ionizing energy 70 eV, ionizing current 0.2 mA, source temperature 250–500 °C). ^{1}H NMR spectra were recorded at 400 MHz on a Bruker WM 400 spectrometer of the Cerema ("Centre de Résonance Magnétique de l'Université de Bourgogne"). Spectra were measured in C_6D_6 or C_4D_8O (0.5 cm^3), and tetramethylsilane was used as an internal reference. Infrared spectra were recorded as a 1% dispersion in CsI pellets. Electronic absorption spectra were obtained on a Perkin-Elmer 559 spectrophotometer or on an IBM Model 9430 spectrophotometer. Cyclic voltammograms were made by using a conventional three-electrode configuration. The working electrode was a platinum button and the counter electrode a platinum wire. A saturated calomel electrode (SCE) was used as the reference electrode and was separated from the bulk of the solution by a fritted-glass bridge. The ferrocene/ferrocenium couple was used as an internal standard for comparing redox potentials of the different (P)Ti(η^2-S_2) and (P)Ti(η^2-Se_2) complexes. A BAS 100 electroanalyzer connected to a Houston Instruments HIPLOT DMP-40 plotter or an IBM 225 voltammetric analyzer connected to a Houston Instruments 2000 X-Y recorder were used to record the current voltage curves. Bulk controlled-potential electrolysis and thin-layer coulommetry were performed with the use of an EG&G Model 173 potentiostat. A EG&G Model 179 X-Y digital coulometer was used to record the current–time curves. Thin-layer spectroelectrochemical measurements were performed with an EG&G Model 173 potentiostat that was coupled with a Tracor Northern 6500 rapid scan spectrometer. The utilized optically transparent platinum thin-layer electrode (OTTLE) has been described in a previous publication.[34] Low-temperature ESR spectra were measured on a Bruker Model 100D ESR spectrometer. Typical temperatures for these measurements were between 173 and 133 K. Tetrabutylammonium perchlorate (TBAP) was used as a supporting electrolyte (0.1 M) for all electrochemical measurements.

X-ray Structure Determination of (TpTP)Ti(η^2-S_2). Suitable crystals for X-ray study of (TpTP)Ti(η^2-S_2) were obtained from recrystallization of the complex in toluene. Weissenberg photographs revealed a monoclinic space group, $P2_1/n$. Crystal data are given in Table I. The data collection was performed at room temperature on an Enraf-Nonius CAD 4 diffractometer using monochromatized Mo Kα radiation. Of 5525 reflections collected up to $(\sin\theta)/\lambda = 0.53$ Å^{-1}, 2858 with $I \geq 3\sigma(I)$ were used to solve and refine the structure. The data reduction was made with the SDP package.[35] The structure was solved by interpretation of the Patterson map and refined via standard least-squares and Fourier tech-

Table I. Crystallographic Data for (TpTP)Ti(η^2-S_2)·$^1/_2C_7H_8$

$C_{48}H_{36}N_4TiS_2 \cdot {}^1/_2C_7H_8$	fw = 826.9
a = 14.688 (2) Å	space group $P2_1/n$ (No. 14)
b = 14.822 (2) Å	λ(Mo Kα) = 0.71073 Å
c = 19.308 (4) Å	d_{calcd} = 1.307 g·cm^{-3}
β = 90.51 (2)°	μ = 2.56 cm^{-1}
V = 4203 Å^3	$R(F_o)$ = 0.047
Z = 4	$R_w(F_o)$ = 0.0494
T = 20 °C	

(10) Carter, M. J.; Rillema, D. P.; Bassolo, F. *J. Am. Chem. Soc.* **1974**, *96*, 392.
(11) Wayland, B. B.; Newman, A. R. *Inorg. Chem.* **1981**, *20*, 3093.
(12) Anderson, J. E.; Yao, C.-L.; Kadish, K. M. *Inorg. Chem.* **1986**, *25*, 3224.
(13) Valentine, J. S. *Chem. Rev.* **1973**, *73*, 235.
(14) Valentine, J. S.; McCandlish, E. In *Frontiers of Biological Energetics*; Dutton, P. L., Leigh, J. S., Scarpa, A., Eds.; Academic Press: New York, 1978; Vol. II, pp 933–940.
(15) McCandlish, E.; Miksztal, A. R.; Nappa, M.; Sprenger, A. Q.; Valentine, J. S. *J. Am. Chem. Soc.* **1980**, *102*, 4268.
(16) Reed, C. A. In *Electrochemical and Spectrochemical Studies of Biological Redox Compounds*; Kadish, K. M., Ed.; Advances in Chemistry Series 201; American Chemical Society: Washington, DC, 1982; p 333 and references therein.
(17) Friant, P.; Goulon, J.; Fisher, J.; Ricard, L.; Shappacher, M.; Weiss, R. *Nouv. J. Chim.* **1985**, *9*, 33.
(18) Miksztal, A. R.; Valentine, J. S. *Inorg. Chem.* **1984**, *23*, 3548.
(19) VanAtta, R. B.; Strouse, C. E.; Hanson, L. K.; Valentine, J. S. *J. Am. Chem. Soc.* **1987**, *109*, 1425.
(20) Chevrier, B.; Diebold, T.; Weiss, R. *Inorg. Chim. Acta* **1976**, *19*, L57.
(21) Deronzier, A.; Latour, J.-M. *Nouv. J. Chim.* **1984**, *8*, 393.
(22) Sakurai, H.; Uchikubo, H.; Ishizu, K.; Tajima, K.; Aoyama, Y.; Ogoshi, H. *Inorg. Chem.* **1988**, *27*, 2691.
(23) Byrn, M. P.; Strouse, C. E. *J. Am. Chem. Soc.* **1981**, *103*, 2633.
(24) Miller, K. M.; Strouse, C. E. *Inorg. Chem.* **1984**, *23*, 2395.
(25) Poncet, J.-L.; Guilard, R.; Friand, P.; Goulon-Ginet, C.; Goulon, J. *Nouv. J. Chim.* **1984**, *8*, 583.
(26) Ratti, C.; Richard, P.; Tabard, A.; Guilard, R. *J. Chem. Soc., Chem. Commun.* **1989**, 69.
(27) The porphyrin rings, P, were the dianions of tetraphenylporphyrin, (TPP), tetra-*m*-tolylporphyrin (TmTP), tetra-*p*-tolylporphyrin (TpTP), tetrakis(*p*-(trifluoromethyl)phenyl)porphyrin ($TpCF_3PP$), tetramesitylporphyrin (TMP), or octaethylporphyrin (OEP).
(28) Guilard, R.; Latour, J.-M.; Lecomte, C.; Marchon, J.-C.; Protas, J.; Ripoll, D. *Inorg. Chem.* **1978**, *17*, 1228.
(29) Malinski, T.; Chang, D.; Latour, J.-M.; Marchon, J.-C.; Gross, M.; Giraudeau, A.; Kadish, K. M. *Inorg. Chem.* **1984**, *23*, 3947.
(30) Fournari, P.; Guilard, R.; Fontesse, M.; Latour, J.-M.; Marchon, J.-C. *J. Organomet. Chem.* **1976**, *110*, 205.
(31) Nakajima, M.; Latour, J.-M.; Marchon, J.-C. *J. Chem. Soc., Chem. Commun.* **1977**, 763.
(32) Latour, J.-M.; Marchon, J.-C.; Nakajima, M. *J. Am. Chem. Soc.* **1979**, *101*, 3974.
(33) Marchon, J. C.; Latour, J. M.; Boreham, C. J. *J. Mol. Catal.* **1980**, *7*, 227.
(34) Lin, X. Q.; Kadish, K. M. *Anal. Chem.* **1985**, *57*, 1498.
(35) *SDP: Structure Determination Package*; Enraf Nonius: Delft, The Netherlands, 1985.

Table II. Positional Parameters and Equivalent Isotropic Temperature Factors of Non-Hydrogen Atoms of (TpTP)Ti(η^2-S_2)

atom	x	y	z	B_{eq},[a] Å^2
Ti	0.41442 (7)	0.37911 (7)	0.63621 (5)	2.65 (2)
S1	0.3883 (1)	0.2668 (1)	0.71448 (9)	4.09 (4)
S2	0.5196 (1)	0.3115 (1)	0.70917 (9)	3.98 (4)
N1	0.2721 (3)	0.3651 (3)	0.6175 (2)	3.1 (1)
N2	0.4279 (3)	0.3089 (3)	0.5436 (2)	3.1 (1)
N3	0.5273 (3)	0.4546 (3)	0.6003 (2)	2.9 (1)
N4	0.3784 (3)	0.4996 (3)	0.6849 (2)	2.9 (1)
C1	0.2044 (4)	0.4000 (4)	0.6591 (3)	3.2 (1)
C2	0.1189 (4)	0.3566 (4)	0.6428 (3)	4.0 (2)
C3	0.1347 (4)	0.2959 (4)	0.5920 (3)	4.1 (2)
C4	0.2309 (4)	0.2994 (4)	0.5768 (3)	3.5 (2)
C5	0.2751 (4)	0.2433 (4)	0.5304 (3)	3.3 (1)
C6	0.3669 (4)	0.2463 (4)	0.5173 (3)	3.3 (2)
C7	0.4154 (4)	0.1849 (5)	0.4723 (3)	4.4 (2)
C8	0.5025 (4)	0.2113 (4)	0.4719 (3)	4.0 (2)
C9	0.5114 (4)	0.2888 (4)	0.5145 (3)	3.3 (2)
C10	0.5882 (4)	0.3421 (4)	0.5198 (3)	3.1 (1)
C11	0.5922 (4)	0.4240 (4)	0.5545 (3)	3.3 (1)
C12	0.6646 (4)	0.4886 (4)	0.5476 (3)	3.7 (2)
C13	0.6445 (4)	0.5572 (4)	0.5914 (3)	3.9 (2)
C14	0.5617 (4)	0.5353 (4)	0.6264 (3)	2.9 (1)
C15	0.5230 (4)	0.5847 (4)	0.6798 (3)	3.2 (1)
C16	0.4376 (4)	0.5658 (4)	0.7084 (3)	2.9 (1)
C17	0.3949 (4)	0.6172 (4)	0.7620 (3)	3.3 (1)
C18	0.3094 (4)	0.5849 (4)	0.7692 (3)	3.8 (2)
C19	0.2983 (4)	0.5117 (4)	0.7214 (3)	3.0 (1)
C20	0.2158 (4)	0.4656 (4)	0.7098 (3)	3.2 (1)
C101	0.6743 (4)	0.3060 (4)	0.4878 (3)	3.6 (2)
C102	0.6928 (5)	0.3142 (5)	0.4184 (3)	5.2 (2)
C103	0.7693 (5)	0.2749 (6)	0.3909 (4)	6.4 (2)
C104	0.8294 (5)	0.2291 (5)	0.4305 (4)	5.8 (2)
C105	0.8117 (6)	0.2236 (6)	0.5006 (4)	7.5 (3)
C106	0.7348 (5)	0.2600 (5)	0.5291 (4)	5.8 (2)
C107	0.9150 (6)	0.1832 (8)	0.3989 (5)	9.7 (3)
C151	0.5756 (4)	0.6632 (4)	0.7077 (3)	3.2 (1)
C152	0.6633 (4)	0.6523 (4)	0.7344 (3)	3.6 (2)
C153	0.7119 (4)	0.7255 (4)	0.7594 (3)	4.1 (2)
C154	0.6763 (4)	0.8124 (4)	0.7584 (3)	4.0 (2)
C155	0.5887 (4)	0.8228 (4)	0.7319 (3)	4.1 (2)
C156	0.5387 (4)	0.7506 (4)	0.7067 (3)	3.6 (2)
C157	0.7291 (5)	0.8940 (5)	0.7851 (4)	6.0 (2)
C201	0.1370 (4)	0.4917 (4)	0.7536 (3)	3.3 (2)
C202	0.0642 (4)	0.5383 (4)	0.7251 (3)	3.9 (2)
C203	−0.0097 (4)	0.5634 (4)	0.7646 (4)	4.4 (2)
C204	−0.0106 (5)	0.5437 (4)	0.8354 (4)	4.8 (2)
C205	0.0619 (5)	0.4986 (5)	0.8634 (4)	5.1 (2)
C206	0.1350 (4)	0.4722 (4)	0.8230 (3)	4.3 (2)
C207	−0.0927 (5)	0.5743 (6)	0.8808 (4)	7.1 (2)
C501	0.2191 (4)	0.1743 (4)	0.4922 (3)	3.6 (2)
C502	0.1983 (5)	0.1860 (5)	0.4236 (3)	5.3 (2)
C503	0.1478 (5)	0.1218 (5)	0.3872 (3)	5.5 (2)
C504	0.1188 (5)	0.0450 (5)	0.4180 (4)	4.9 (2)
C505	0.1370 (6)	0.0345 (5)	0.4860 (4)	7.4 (3)
C506	0.1876 (6)	0.0978 (5)	0.5232 (4)	6.1 (2)
C507	0.0623 (6)	−0.0241 (6)	0.3771 (4)	7.8 (3)
C21	0.507 (1)	0.1021 (9)	−0.0414 (8)	9*
C22	0.582 (1)	0.0526 (9)	−0.0642 (8)	9*
C23	0.595 (1)	−0.0357 (9)	−0.0413 (8)	9*
C24	0.533 (1)	−0.0745 (9)	0.0045 (8)	9*
C25	0.458 (1)	−0.0250 (9)	0.0273 (8)	9*
C26	0.445 (1)	0.0633 (9)	0.0044 (8)	9*
C27	0.397 (2)	−0.070 (2)	0.079 (1)	12*

[a] Starred *B* values are for atoms that were constrained to isotropic thermal motion.

niques (SHELX 76).[36] All non-hydrogen atoms of the complex were refined anisotropically. The hydrogen atoms attached to trigonal carbon atoms were included in calculated positions (1.07 Å from the bonded atom) and allowed to ride on that atom with *B* fixed to 1.3 times those of the corresponding carbon atom. During refinement, difference electron density maps showed a large region of positive electron density near the [$^1/_2$, 0, 0] inversion center. This was interpretated as a disordered toluene solvation molecule in two different positions related by the inversion center. During refinement, the geometry of the six atoms of the toluene ring (C21–C26) was idealized (C–C = 1.40 (1) Å, C–C–C = 120 (1)°, fixed occupancy m = 0.5). The methyl group was included in the refinement and constrained to give a bond length of 1.50 Å and a fixed occupancy m = 0.5. These atoms were isotropically refined. Final difference Fourier map showed a residual electron density of 0.3 e/Å^3, which probably corresponds to a hydrogen atom of a methyl group of the porphyrin. Final residuals were $R(F_o)$ = 4.7%, $R_w(F_o)$ = 4.94%, and GOF = 1.35. The scattering factors were taken from ref 37. Fractional coordinates of the non-hydrogen atoms of (TpTP)Ti(η^2-S_2) are given in Table II, and main bond distances and angles are given in Table III. A list of other bond distances and angles, anisotropic thermal parameters, hydrogen coordinates, least-squares planes, experimental conditions, and structure factors are given as supplementary material.

Table III. Bond Distances (Å) and Angles (deg) in the Coordination Polyhedron of (TpTP)Ti(η^2-S_2)

Bond Distances			
Ti–S1	2.283 (2)	Ti–N3	2.121 (4)
Ti–S2	2.311 (2)	Ti–N4	2.089 (5)
Ti–N1	2.129 (5)	S1–S2	2.042 (2)
Ti–N2	2.080 (4)		
Bond Angles			
S1–Ti–S2	52.78 (6)	N1–Ti–N4	84.7 (2)
Ti–S1–S2	64.30 (7)	N2–Ti–N3	84.4 (2)
Ti–S2–S1	62.92 (8)	N2–Ti–N4	147.3 (2)
N1–Ti–N2	84.5 (2)	N3–Ti–N4	84.1 (2)
N1–Ti–N3	139.9 (2)		

Results and Discussion

Characterization of Neutral (P)Ti(η^2-Y_2). Elemental analysis and mass spectral data of the synthesized complexes are summarized in Tables IV and V and are in good agreement with (P)Ti(η^2-S_2) or (P)Ti(η^2-Se_2) as the molecular formula. The fragmentation patterns listed in Table V are only those of the major ^{48}Ti and ^{80}Se isotopes which are in 73.8 and 49.6% abundance, respectively.

The [(P)Ti(η^2-S_2)]$^{\bullet+}$ molecular peak varies between 15.30 and 72.30% in relative intensity and is stronger than the analogous diselenium species, [(P)Ti(η^2-Se_2)]$^{\bullet+}$, which varies from 4.50 to 36.60%. The only exception is for the two (TpCF$_3$PP)Ti(η^2-Y_2) derivatives, and the overall data thus suggest that the Ti–S bonds in (P)Ti(η^2-S_2) are stronger than the Ti–Se bonds in (P)Ti(η^2-Se_2).

The parent peaks of (P)Ti(η^2-S_2) and (P)Ti(η^2-Se_2) are [(P)TiS]$^+$ and [(P)TiSe]$^+$, but a high-intensity peak corresponding to [(P)Ti]$^+$ is also present for both compounds. This fragmentation pattern implies a rupture of both the titanium–chalcogen and the chalcogen–chalcogen bonds of the initial complex. A similar pattern is not observed for (TpCF$_3$PP)Ti(η^2-S_2) which has [(TpCF$_3$PP)Ti(S_2) + H]$^+$ as the parent peak. The mass spectral data for (P)Ti(η^2-S_2) and (P)Ti(η^2-Se_2) are similar to mass spectral data for (P)Ti(η^2-O_2), which has also [(P)TiO]$^+$ as the parent peak.[28]

Infrared data for the chalcogen ligand of each (P)Ti(η^2-S_2) complex are listed in Table VI, while Figure 1a illustrates the IR spectrum of (TPP)Ti(η^2-S_2). This compound has an S–S vibration at 551 cm^{-1} in CsI pellets, and the other (P)Ti(η^2-S_2) compounds have the strong vibrational band of the S_2 ligand between 549 and 553 cm^{-1}. These values are also similar to those of non-porphyrin disulfur organometallic complexes,[3,38–43] which have a cis-hexacoordination scheme of the ligand and show S–S vibrations between 510 and 558 cm^{-1}. Comparison of the ν(S–S) frequencies for free S_2 (725 cm^{-1}) and ionic S_2^- (589 cm^{-1}) and S_2^{2-} (446

(36) Sheldrick, G. M. *SHELX 76, Program for Crystal Structure Determinations*; University of Göttingen: Gottingen, West Germany, 1976.
(37) *International Tables for X-Ray Crystallography*; Kynoch: Birmingham, U.K., 1974; Vol. IV.
(38) Koch, S. A.; Chebolu, V. *Organometallics* **1983**, *2*, 350.
(39) Treichel, P. M.; Werber, G. P. *J. Am. Chem. Soc.* **1968**, *90*, 1753.
(40) Bond, A. M.; Broomhead, J. A.; Hollenkamp, A. F. *Inorg. Chem.* **1988**, *27*, 978.
(41) Farrar, D. H.; Grundy, K. R.; Payne, N. C.; Roper, W. R.; Walker, A. *J. Am. Chem. Soc.* **1979**, *101*, 6577.
(42) Ginsberg, A. P.; Lindsell, W. E.; Sprinkle, C. R.; West, K. W.; Cohen, R. L. *Inorg. Chem.* **1982**, *21*, 3666.
(43) Müller, A.; Jaegermann, W. *Inorg. Chem.* **1979**, *18*, 2631.

Table IV. Yields[a] and Elemental Analyses of (P)Ti(Y_2), Where Y = S or Se

porphyrin, P	axial ligand, Y	recryst solvent[b]	yield, %	molec formula	elemental anal., %[c] C	H	N	Ti	Y
TPP	S	A	64	$C_{44}H_{28}N_4TiS_2$	69.8 (72.91)	3.9 (3.90)	7.1 (7.73)	6.3 (6.61)	8.7 (8.85)
TmTP		B	77	$C_{48}H_{36}N_4TiS_2$	73.4 (73.82)	4.8 (4.66)	7.0 (7.18)	5.7 (6.13)	7.7 (8.21)
TpTP		A	83	$C_{48}H_{36}N_4TiS_2$	73.7 (73.82)	4.7 (4.66)	7.0 (7.18)	5.6 (6.13)	7.7 (8.21)
$TpCF_3PP$[d]		A	88	$C_{48}H_{24}N_4F_{12}TiS_2$	60.2 (57.84)	2.9 (2.43)	5.0 (5.62)	4.8 (4.81)	5.6 (6.43)
TMP		A	71	$C_{56}H_{52}N_4TiS_2$	76.0 (75.30)	6.1 (5.88)	5.2 (6.27)	4.6 (5.36)	6.1 (7.18)
OEP		A/B (3/1)	69	$C_{36}H_{44}N_4TiS_2$	68.1 (67.04)	7.0 (6.89)	7.8 (8.69)	6.9 (7.43)	9.1 (9.95)
TPP	Se	A/B (2/1)	58	$C_{44}H_{28}N_4TiSe_2$	67.6 (64.55)	3.6 (3.45)	6.7 (6.85)	5.7 (5.85)	23.2 (19.29)
TmTP		A/B (1/3)	74	$C_{48}H_{36}N_4TiSe_2$	64.6 (65.90)	4.3 (4.16)	6.1 (6.41)	5.3 (5.46)	18.8 (18.05)
TpTP		A/B (2/1)	61	$C_{48}H_{36}N_4TiSe_2$	57.8 (65.90)	4.2 (4.16)	5.4 (6.41)	5.0 (5.46)	17.4 (18.05)
$TpCF_3PP$[e]		A	68	$C_{48}H_{24}N_4F_{12}TiSe_2$	52.9 (52.86)	2.2 (2.22)	5.2 (5.14)	4.2 (4.39)	14.6 (14.48)
TMP		A	85	$C_{56}H_{52}N_4TiSe_2$	69.1 (68.14)	5.7 (5.32)	4.8 (5.68)	4.1 (4.85)	13.6 (16.00)
OEP		A	69	$C_{36}H_{44}N_4TiSe_2$	58.1 (58.53)	5.8 (6.02)	6.7 (7.59)	5.1 (6.48)	18.6 (21.38)

[a] Yields from syntheses by method A (see experimental section). [b] Solvents: A, toluene; B, heptane. [c] Calculated values are in parentheses. [d] Fluorine analysis: 21.1% (22.87%). [e] Fluorine analysis: 20.1% (20.91%).

Table V. Mass Spectral Data for (P)Ti(S_2) and (P)Ti(Se_2)

porphyrin, P	(P)Ti(S_2) *m/e*	rel intens, %	fragmentn pattern	(P)Ti(Se_2) *m/e*	rel intens, %	fragmentn pattern
TPP	724	32.40	$[(TPP)Ti(S_2)]^{+\cdot}$	820	18.20	$[(TPP)Ti(Se_2)]^{+\cdot}$
	692	100.00	$[(TPP)TiS]^+$	740	100.00	$[(TPP)TiSe]^+$
	660	41.70	$[(TPP)Ti]^+$	660	67.60	$[(TPP)Ti]^+$
TmTP	780	58.60	$[(TmTP)Ti(S_2)]^{+\cdot}$	876	26.60	$[(TmTP)Ti(Se_2)]^{+\cdot}$
	748	100.00	$[(TmTP)TiS]^+$	796	100.00	$[(TmTP)TiSe]^+$
	716	50.00	$[(TmTP)Ti]^+$	716	92.40	$[(TmTP)Ti]^+$
TpTP	780	37.90	$[(TpTP)Ti(S_2)]^{+\cdot}$	876	29.70	$[(TpTP)Ti(Se_2)]^{+\cdot}$
	748	100.00	$[(TpTP)TiS]^+$	796	100.00	$[(TpTP)TiSe]^+$
	716	38.60	$[(TpTP)Ti]^+$	716	94.70	$[(TpTP)Ti]^+$
$TpCF_3PP$	997	100.00	$[(TpCF_3PP)Ti(S_2) + H]^+$	1093	10.00	$[(TpCF_3PP)Ti(Se_2) + H]^+$
	996	15.30	$[(TpCF_3PP)Ti(S_2)]^{+\cdot}$	1092	36.60	$[(TpCF_3PP)Ti(Se_2)]^{+\cdot}$
	964	2.50	$[(TpCF_3PP)TiS]^+$	1012	100.00	$[(TpCF_3PP)TiSe]^+$
	932	77.50	$[(TpCF_3PP)Ti]^+$	932	52.70	$[(TpCF_3PP)Ti]^+$
TMP	892	35.80	$[(TMP)Ti(S_2)]^{+\cdot}$	988	4.50	$[(TMP)Ti(Se_2)]^{+\cdot}$
	860	100.00	$[(TMP)TiS]^+$	908	32.00	$[(TMP)TiSe]^+$
	847	43.00	$[(TMP)TiS - CH_3 + 2H]^+$	828	34.00	$[(TMP)Ti]^+$
	828	24.80	$[(TMP)Ti]^+$			
OEP	644	72.30	$[(OEP)Ti(S_2)]^{+\cdot}$	740	14.86	$[(OEP)Ti(Se_2)]^{+\cdot}$
	612	100.00	$[(OEP)TiS]^+$	660	100.00	$[(OEP)TiSe]^+$
	580	49.10	$[(OEP)Ti]^+$	580	43.50	$[(OEP)Ti]^+$

Table VI. IR Data for (P)Ti(S_2) and (P)Ti(Se_2)

porphyrin, P	ν, cm^{-1} S–S	Se–Se	Ti–S	Ti–Se
TPP	551	440	426	407
TmTP	551	435	426	408
TpTP	549	433	429	407
$TpCF_3PP$	551	436	432	*a*
TMP	553	*a*	429	404
OEP	549	*a*	420	400

[a] Peak not observed.

cm^{-1})[3] indicates that the S–S bond strength of the (P)Ti(η^2-S_2) complexes lies between that of ionic S_2^- and S_2^{2-}. No significant changes in S–S frequencies of (P)Ti(η^2-S_2) are observed with changes in the porphyrin macrocycle.

The Ti(IV) central metal and the two sulfur atoms of (P)Ti(η^2-S_2) fit into a triangular structure. There is only one Ti–S vibration for (TPP)Ti(η^2-S_2), and this occurs at 426 cm^{-1} (see Figure 1a). The Ti–S vibrations of the other complexes range between 420 and 432 cm^{-1} (see Table VI) and are higher than the Ti–S vibrations of other sulfur-containing organometallic compounds, which have metal–sulfur vibrations between 321 and 386 cm^{-1}.[3] The higher wavenumbers for (P)Ti(η^2-S_2) result from the fact that the porphyrin macrocycle induces longer Ti–S bond distances.

The IR spectrum of (TPP)Ti(η^2-Se_2) in CsI pellets is shown in Figure 1b, and the Se–Se and Ti–Se vibrations of the various

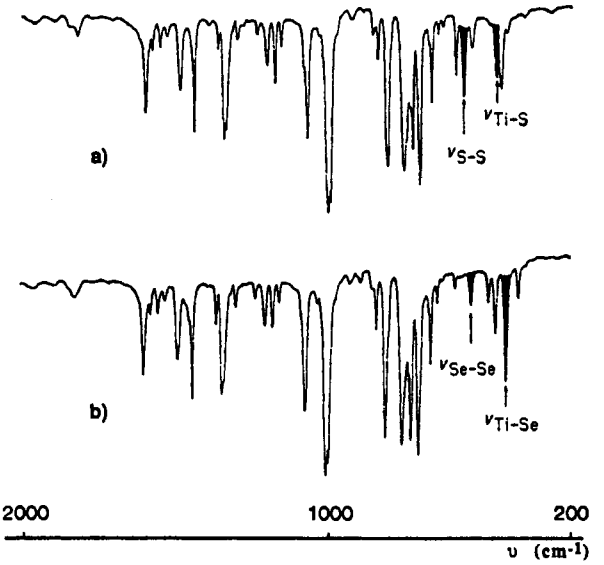

Figure 1. IR spectra of (a) (TPP)Ti(η^2-S_2) and (b) (TPP)Ti(η^2-Se_2) in CsI pellets.

complexes are summarized in Table VI. The Se–Se vibrations of (TMP)Ti(η^2-Se_2) and (OEP)Ti(η^2-Se_2) cannot be detected in the IR spectrum. However, the other four complexes have an Se–Se vibration between 433 and 440 cm^{-1}, and this is in

Table VII. UV–Visible Data for (P)Ti(Y_2), Where Y = S or Se in Toluene

porphyrin, P	ax ligand, Y	λ_{max}, nm ($10^{-3}\epsilon$, $M^{-1}\cdot cm^{-1}$) band I	band II[a]	Q(2,0)	Q(1,0)	Q(0,0)	ϵ(II)/ϵ(I)
TPP	S	378 (29.8)	430 (107.6)		546 (10.9)	631 (2.4)	3.70
TmTP		378 (30.5)	430 (125.8)		547 (11.2)	630 (2.0)	4.17
TpTP		379 (28.5)	432 (121.9)		549 (10.3)		4.35
$TpCF_3PP$		372 (32.4)	429 (135.4)		545 (11.7)	630 (1.9)	4.17
TMP		379 (36.7)	431 (139.9)		548 (13.7)		3.85
OEP		363 (26.8)	417 (33.1)	536 (6.1)	574 (9.8)	632 (1.5)	1.23
TPP	Se	389 (52.6)	434 (98.9)		547 (11.1)	631 (1.0)	1.89
TmTP		388 (55.7)	435 (104.4)		547 (11.8)	631 (1.1)	1.89
TpTP		389 (51.7)	437 (103.6)		548 (10.6)		2.00
$TpCF_3PP$		384 (52.6)	432 (112.2)		544 (12.9)	630 (1.0)	2.13
TMP		388 (46.7)	435 (86.7)		548 (11.7)		1.85
OEP[b]		376 (67.1)	421 (41.3)	538 (8.0)	576 (14.8)		0.62

[a] Band B(0,0). [b] In tetrahydrofuran solution.

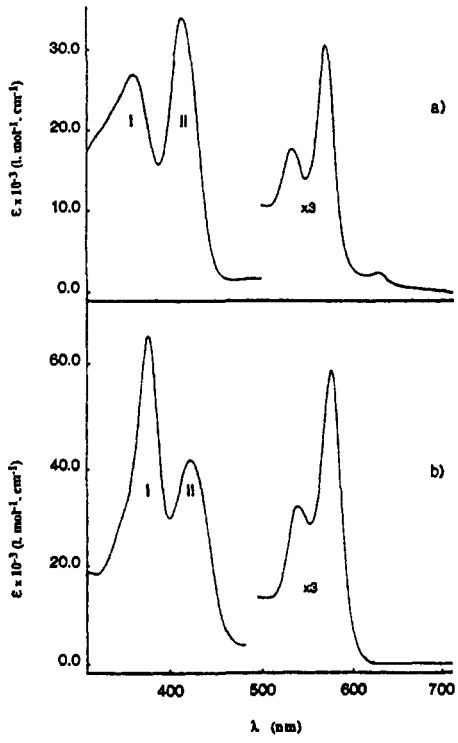

Figure 2. UV–visible spectra of (a) (OEP)Ti(η^2-S_2) in toluene and (b) (OEP)Ti(η^2-Se_2) in tetrahydrofuran.

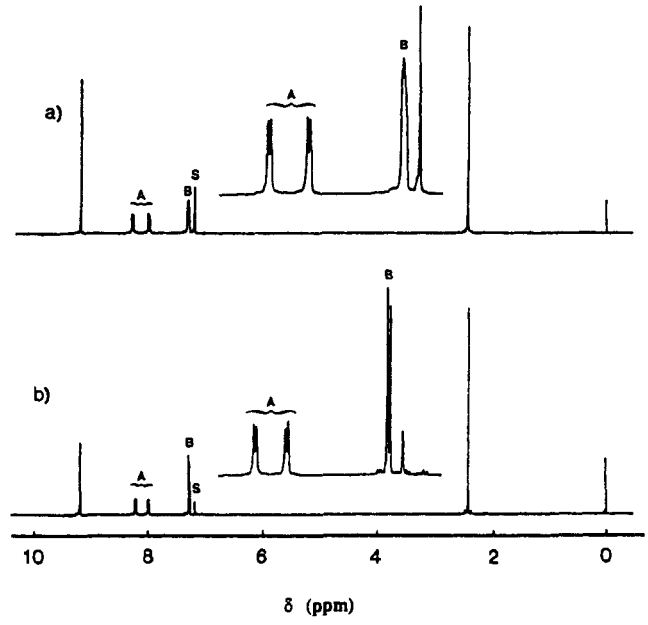

Figure 3. ^{1}H NMR spectra of (a) (TpTP)Ti(η^2-S_2) and (b) (TpTP)-Ti(η^2-Se_2) in C_6D_6 at 294 K. The symbol "s" indicates signals for the solvent molecules.

agreement with a coordination scheme where the Se_2 ligand is "side-on" bonded to the Ti(IV) metal center. These wavenumbers are higher than those of the Se_2^- anion (325 cm^{-1})[42] and suggest a similar charge distribution as in the disulfur complexes.

The Se–Se vibrations in Table VI can be compared with vibrations of non-porphyrin organometallic selenium derivatives, which range between 300 and 310 cm^{-1},[38-42] and the data suggest a deformation of the Ti(η^2-Se_2) group of (P)Ti(η^2-Se_2). The larger size of the selenium atom compared to sulfur implies a large steric constraint of Se_2 in (P)Ti(η^2-Se_2).

Figure 2 shows the UV–visible spectra of (OEP)Ti(η^2-S_2) and (OEP)Ti(η^2-Se_2), while data for each of the (P)Ti(η^2-S_2) and (P)Ti(η^2-Se_2) complexes are summarized in Table VII. These spectra can be characterized as belonging to the hyperporphyrin class in that they exhibit two bands in the Soret region.[44] These bands are labeled as bands I and II in Table VII and in Figure 2.

Wavelength maxima of the B(0,0) absorptions (band II) are close to those of low-valent titanium(III) complexes that have the same porphyrin ring,[33] and this suggests that there is a large charge delocalization from the axial disulfur or diselenium ligand of (P)Ti(S_2) or (P)Ti(Se_2) to the central metal. The "extra" band I may result from a charge transfer from the axial ligand to titanium (π_z^*) → (3d).

The ratio of molar absorptivities between bands I and II, ϵ-(II)/ϵ(I), depends upon the specific equatorial and/or axial ligand and varies from 0.62 for (OEP)Ti(η^2-Se_2) to 4.35 for (TpTP)-Ti(η^2-S_2). The smallest ratios in a given S_2 or Se_2 series are obtained for the OEP complexes, while for a given porphyrin macrocycle, smaller values are obtained for (P)Ti(η^2-Se_2) rather than (P)Ti(η^2-S_2) (see Table VII). These differences in ϵ(II)/ϵ(I) can be explained by the larger electron-donating properties of selenium compared to sulfur and the larger electron-donating properties of OEP compared to the other porphyrin macrocycles. This also indicates more covalent metal–axial ligand bonds for the (OEP)Ti(η^2-Se_2) complex and agrees with the lower Ti–S and Ti–Se vibration frequencies of the octaethylporphyrin complexes (see Table VI).

Typical ^{1}H NMR spectra for (TpTP)Ti(η^2-S_2) and (TpTP)-Ti(η^2-Se_2) at 294 K in C_6D_6 are shown in Figure 3. Chemical shifts of the compounds are summarized in Table VIII and are characteristic of diamagnetic porphyrins. These data suggest that the titanium metal is in a +4 oxidation state.[45] The pyrrolic proton peak of the tetraarylporphyrin derivatives is located between

(44) Gouterman, M. In *The Porphyrins*; Dolphin, D., Ed.; Academic: New York, 1978; Vol. III, Chapter 1.

(45) Janson, T. R.; Katz, J. J. In *The Porphyrins*; Dolphin, D., Ed.; Academic: New York, 1978; Vol. IV, Chapter 1.

Table VIII. ^{1}H NMR Spectroscopic Data of (P)Ti(Y_2), Where Y = S or Se in C_6D_6 Solution at 294 K

porphyrin, P	ax ligand, Y	pyr H		*o*-H		*m*-H		*p*-H		*o*-CH_3		*m*-CH_3		*p*-CH_3		*meso*-H		α-CH_2		β-CH_3	
		δ^a	m/i^b	δ^a	m/i^b	δ^a	m/i^b	δ^a	m/i^b	δ^a	m/i^b	δ^a	m/i^b	δ^a	m/i^b	δ^a	m/i^b	δ^a	m/i^b	δ^a	m/i^b
TPP	S	8.98	s/8	8.14	d/4		7.43	m/12													
				7.96	d/4																
	Se	8.96	s/8	8.17	d/4		7.46	m/12													
				7.94	d/4																
TmTP	S	9.08	s/8	8.11	m/2	7.38	m/4	7.34	m/4			2.29	s/6								
				8.06	d/2							2.31	s/6								
				7.88	d/2																
				7.82	m/2																
	Se	9.06	s/4	8.16	m/2	7.38	m/4	7.33	m/4			2.30	s/12								
		9.05	s/4	8.09	d/2																
				7.86	d/2																
				7.79	m/2																
TpTP	S	9.11	s/8	8.12	d/4	7.25	m/8							2.38	s/12						
				7.91	d/4																
	Se	9.04	s/8	8.15	d/4	7.26	m/8							2.33	s/12						
				7.90	d/4																
Tp-CF_3PP	S	8.79	s/8	7.96	d/4	7.66	m/8														
				7.78	d/4																
	Se	8.77	s/8	8.00	d/4	7.66	m/8														
				7.76	d/4																
TMP	S	8.93	s/8			7.11	s/4			2.05	s/12			2.41	s/12						
						7.08	s/4			1.78	s/12										
	Se	8.91	s/8			7.15	s/4			2.15	s/12			2.41	s/12						
						7.10	s/4			1.71	s/12										
OEP	S															10.50	s/4	4.00	m/8	1.78	1/24
																		3.86	m/8		
	Se															10.40	s/4	4.00	m/8	1.77	t/24
																		3.84	m/8		

^{a} δ, ppm. ^{b} m/i = multiplicity/intensity; s = singlet; d = doublet, t = triplet; m = multiplet.

Table IX. ^{1}H NMR Chemical Shifts^a of Tetraaryl Derivative Ortho Protons in C_6D_6 at 294 K

compd	δ(*o*-H)	δ(*o*-H)	Δ^b
(TPP)Ti(S_2)	8.14	7.96	0.18
(TmTP)Ti(S_2)	8.11	7.88	0.23
(TpTP)Ti(S_2)	8.12	7.91	0.21
(TpCF_3PP)Ti(S_2)	7.96	7.78	0.18
(TPP)Ti(Se_2)	8.17	7.94	0.23
(TmTP)Ti(Se_2)	8.16	7.86	0.30
(TpTP)Ti(Se_2)	8.15	7.91	0.25
(TpCF_3PP)Ti(Se_2)	8.01	7.76	0.24

^{a} In ppm with respect to the TMS internal reference (C_6D_6, 294 K). ^{b} Δ = δ(*o*-H) − δ(*o*′-H) in ppm.

8.79 and 9.11 ppm for the S_2 complexes and between 8.77 and 9.06 ppm for the Se_2 species. Complexes with diselenium ligands are at higher fields than those with disulfur ligands, and this agrees with the UV–visible data, which also show the higher electron-donating properties of the Se_2^{2-} ligand compared to S_2^{2-}.

The ortho protons of the porphyrin ligand appear as two doublets in the range 7.78–8.14 ppm for the perthio tetraaryl complexes. These signals are located between 7.76 and 8.17 ppm for the diselenium derivatives. The differences between the *o*-H and *o*′-H resonance frequencies of the tetraarylporphyrin macrocycles are given in Table IX and involve a dissymmetry with respect to the porphyrin plane. This anisotropy agrees with a cis-hexacoordinated Ti(IV) central metal. A comparison of the ^{1}H NMR data in Tables VIII and IX with similar data for (P)TiO and (P)Ti(η^2-O_2)[28] implies a larger dissymmetry of the (P)Ti(η^2-S_2) and (P)Ti(η^2-Se_2) complexes. This is confirmed by the separation of the α-CH_2 resonances into two multiplets arising from an ABX_3 coupling with the β-CH_3 group for the two OEP derivatives. The *o*-methyl protons of (TMP)Ti(η^2-S_2) appear as two singlets at 1.78 and 2.05 ppm, while (TMP)Ti(η^2-Se_2) has two singlets at 1.71 and 2.15 ppm. This result is consistent with a bulkiness of the complexes in the TMP series and with a restricted rotation of the aryl rings.

The corresponding resonances of (TmTP)Ti(η^2-S_2) and (TmTP)Ti(η^2-Se_2) are more complicated. The ^{1}H NMR spectrum

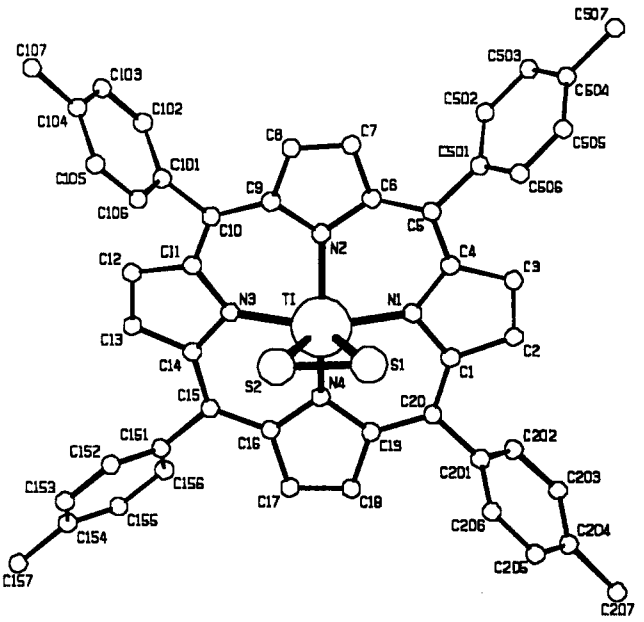

Figure 4. PLUTO view of (TpTP)Ti(η^2-S_2).

of (TmTP)Ti(η^2-S_2) shows four very well separated peaks: two doublets at 7.88 and 8.06 ppm and two broad signals at 7.82 and 8.11 ppm. The analogous (TmTP)Ti(η^2-Se_2) derivative has two doublets at 7.86 and 8.09 ppm and two broad signals at 7.79 and 8.16 ppm. The steric constraint created between the *m*-tolyl groups of the porphyrin ring and the Ti(η^2-S_2) or the Ti(η^2-Se_2) moiety can account for the complexity of the *o*-hydrogen resonances of these two porphyrins. The ^{1}H NMR high-temperature spectra give a coalescence temperature close to 363 K for the ortho protons.

X-ray Molecular Structure of (TpTP)Ti(η^2-S_2). The preliminary X-ray structure of (TpTP)Ti(η^2-S_2) has been briefly described in a previous publication.[26] The PLUTO view of the molecule is shown in Figure 4, while Table III gives the main bond lengths

Table X. Half-Wave and Peak Potentials (V vs SCE) for the Reduction and Oxidation of (P)Ti(Y_2), Where Y = S or Se in CH_2Cl_2, 0.1 M TBAP (Scan Rate = 0.1 V/s)

porphyrin, P	ax ligand, Y	redn $E_{1/2}$	redn $E_{1/2}$	oxidn E_p
TPP	S	−1.05	−1.40	0.98
	Se	−1.06	−1.44	0.77
TmTP	S	−1.07	−1.43	1.00
	Se	−1.06	−1.42	0.82
TpTP	S	−1.04	−1.38	0.98
	Se	−1.06	−1.39	0.80
$TpCF_3PP$	S	−0.91	−1.26	1.12
	Se	−0.90	−1.28	0.97
TMP	S	−1.18	−1.61	1.05
	Se	−1.21	−1.71	0.89
OEP	S	−1.26	−1.62	0.88
	Se	−1.26	−1.63	0.69

and angles. The S_2 group is η^2 "side-on" bonded to the titanium atom and eclipses two opposite nitrogen atoms N1 and N3. This coordination scheme is similar to that of the peroxo analogue, (OEP)Ti(η^2-O_2).[28] As expected for such a coordination scheme, two different metal–nitrogen atom distances are found: Ti–N1 = 2.129 (5) Å, Ti–N3 = 2.121 (4) Å and Ti–N2 = 2.080 (4) Å, Ti–N4 = 2.089 (5) Å. The Ti–S bond distances are Ti–S1 = 2.283 (2) Å and Ti–S2 = 2.311 (2) Å. Molecular orbital calculations[46] on the peroxo derivatives have been used to explain this eclipsed conformation by a bonding interaction between the d_{xy} metal orbital with a π^* molecular orbital of the η^2 diatomic ligand ($\pi^* \rightarrow d_{xy}$). The same electronic effect can be invoked for the dithioporphyrin complexes. Moreover, the S–S distance of 2.042 (2) Å is close to distances found in other η^2-S_2-coordinated compounds[3] and should be compared with values found for free S_2 (1.89 Å) or ionic S_2^- (2.00 Å) and S_2^{2-} (2.13 Å).[3] The rather short S–S distance value compared to that of S_2^{2-} for (TpTP)Ti(η^2-S_2) is consistent with some charge delocalization from the S_2^{2-} ligand to the metal and is in good agreement with the measured S–S vibrational frequency. The titanium atom lies 0.658 (1) Å above the plane of the four nitrogen atoms. This distance is slightly larger than the corresponding distance observed for the peroxo derivative [Δ4N = 0.620 (6) Å].[28]

Electroreduction of (P)Ti(η^2-S_2) and (P)Ti(η^2-Se_2). The investigated perseleno and perthio derivatives exhibit similar electrochemical behavior by cyclic voltammetry. Each of the 12 species undergoes two reversible reductions between −0.90 and −1.71 V in CH_2Cl_2, 0.1 M TBAP and one or more oxidations at potentials positive of 0.69 V (Table X). Cyclic voltammograms of (P)Ti(η^2-S_2) and (P)Ti(η^2-Se_2) (P = TpTP, OEP) are shown in Figure 5. The values of $E_{1/2}$ for reduction of (P)Ti(η^2-S_2) and (P)Ti(η^2-Se_2) are similar for a given porphyrin macrocycle P, and this suggests an electrode reaction that occurs at the porphyrin π ring system rather than at the central metal ion or at the axial ligand.

Each reduction of (P)Ti(η^2-S_2) or (P)Ti(η^2-Se_2) involves a diffusion-controlled reversible to quasireversible one-electron transfer process. The peak currents are proportional to the square root of scan rate, and the anodic to cathodic peak separations are 65 ± 5 mV for the first reduction and 85 ± 10 mV for the second reduction at a scan rate of 0.1 V/s.

The absolute potential difference between the two reductions is 0.36 ± 0.03 V for 10 of the 12 compounds, but (TMP)Ti(η^2-S_2) and (TMP)Ti(η^2-Se_2) show larger separations of 0.43 and 0.50 V, respectively (see Table X). The values of 0.36 ± 0.03 V are somewhat smaller than the 0.42 ± 0.05 V generally observed for ring-centered reductions of metalloporphyrins,[47] but as will be shown, these reactions occur at the porphyrin π ring system.

The values of $E_{1/2}$ for reduction of (P)Ti(η^2-S_2) or (P)Ti(η^2-Se_2) are also similar to values for reduction of (P)TiO under similar experimental conditions as reported in the literature[29] or as measured in this present study.[48] A similar first reduction potential is also found for (P)Ti(η^2-O_2) in CH_2Cl_2,[29] but the overall electrochemical behavior of (P)Ti(η^2-Y_2), where P = OEP or TPP and Y = S or Se, differs from the analogous (P)Ti(η^2-O_2) complexes, where P = OEP or TPP. The first reduction of the peroxo derivatives leads to the corresponding oxo porphyrin,[29] but this is not the case for the perthio or perseleno porphyrins, which form stable π anion radicals in CH_2Cl_2.

The voltammograms of (OEP)Ti(η^2-S_2) and (OEP)Ti(η^2-Se_2) are similar to those of (TpTP)Ti(η^2-S_2) and (TpTP)Ti(η^2-Se_2) (see Figure 5), but additional electrochemical data indicate that the OEP complexes are unstable upon the bulk controlled-potential electrolysis time scale. Thin-layer electrolysis combined with spectroelectrochemistry and coulometry shows that the first reduction of (OEP)Ti(η^2-S_2) and (OEP)Ti(η^2-Se_2) involves a

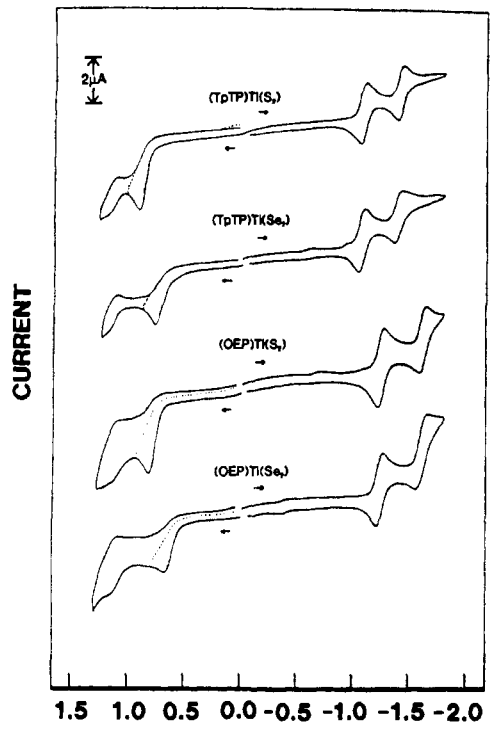

Figure 5. Cyclic voltammograms of (TpTP)Ti(η^2-S_2), (TpTP)Ti(η^2-Se_2), (OEP)Ti(η^2-S_2), and (OEP)Ti(η^2-Se_2) in CH_2Cl_2, 0.1 M TBAP at a scan rate of 0.1 V/s.

Table XI. Maximum Absorbance Wavelengths (λ_{max}) and Corresponding Molar Absorptivities (ϵ) of Neutral and Reduced (P)Ti(S_2) and (P)Ti(Se_2) Complexes in CH_2Cl_2, 0.1 M TBAP

compd	λ_{max}, nm ($10^4\epsilon$, $M^{-1}\cdot cm^{-1}$) neutral		reduced	
(TPP)Ti(S_2)	390 (39)	423 (145)	396 (sh)	444 (77)
	548 (14)			687 (8)
(TpTP)Ti(S_2)	390 (59)	431 (146)	396 (47)	447 (86)
	550 (17)	627 (6)	632 (14)	675 (14)
			793 (6)	
($TpCF_3PP$)Ti(S_2)	380 (53)	424 (179)	388 (53)	445 (90)
	548 (19)	628 (7)	635 (13)	672 (13)
(TpTP)Ti(Se_2)	396	428,[a] 435	397	427,[a] 443
	548		635	691

[a] Band due to traces of (TpTP)TiO in original compound.

(46) Dedieu, A.; Rohmer, M.-M.; Veillard, H.; Veillard, A. *Nouv. J. Chim.* **1979**, *3*, 653.
(47) Kadish, K. M. *Prog. Inorg. Chem.* **1986**, *34*, 435.
(48) Half-wave potentials for the reductions of (P)TiO in CH_2Cl_2, 0.1 M TBAP as measured in our laboratory are as follows: (TpTP)TiO, $E_{1/2}$ = −1.10 and −1.48 V; (TmTP)TiO, $E_{1/2}$ = −1.09 and −1.47 V; ($TpCF_3PP$)TiO, $E_{1/2}$ = −0.94 and −1.32 V; (TMP)TiO, $E_{1/2}$ = −1.24 and −1.73 V.

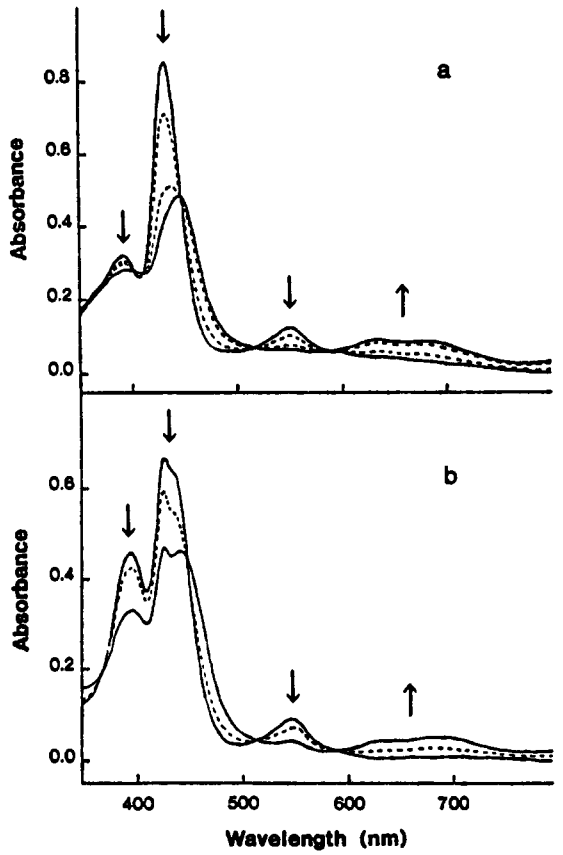

Figure 6. Time-resolved electronic absorption spectra taken during reduction of (a) (TpTP)Ti(η^2-S_2) and (b) (TpTP)Ti(η^2-Se_2) in CH_2Cl_2, 0.1 M TBAP at an applied potential of −1.20 V. Spectra were taken at (a) t = 0, 10, 30, and 70 s and (b) t = 0, 10, and 35 s.

multistep phenomenon yielding nonidentifiable products after the addition of numerous electrons.

Spectroelectrochemistry of (P)Ti(η^2-S_2) and (P)Ti(η^2-Se_2). Spectral changes recorded during time-resolved thin-layer electrolysis of (TpTP)Ti(η^2-S_2) at −1.2 V are shown in Figure 6, while the maximum wavelengths and molar absorptivities for three of the electrogenerated products are reported in Table XI. The blue-shifted extra absorption band of the neutral complexes is located in the range 380–396 nm and changes little after reduction. However, other parts of the spectra undergo dramatic changes upon reduction of the complex by one electron. For example, as seen in Figure 6, the B(0,0) band of the neutral species decreases and is replaced by a new band between 443 and 447 nm. At the same time, the Q(1,0) band totally disappears and two new bands appear between 632 and 691 nm. Isosbestic points are observed during the initial 2 min of electrolysis. In addition, these spectral changes are reversible at short electrolysis times. This was demonstrated by the fact that the original spectrum could be regenerated when the potential was reset to 0.0 V.

The spectra of the reduction products (see Table XI) are characteristic of porphyrin π anion radicals in that they have a decreased Soret band intensity and broad absorptions between 600 and 750 nm. The spectral data for these species are also similar to spectral data for singly reduced (TPP)TiO but values of ϵ and λ obtained in this present study[49] deviate from data previously reported under the same experimental conditions.[29]

Coulometric reduction of (P)Ti(η^2-S_2) (P = TPP, TpTP, $TpCF_3PP$) at potentials negative of $E_{1/2}$ give values of 1.0 ± 0.1 electrons/molecule. The generated green species exhibits a strong symmetrical ESR signal at low temperature and is centered at g = 2.002 ± 0.001. These g values are characteristic of porphyrin π anion radicals and can be compared to g = 2.007 for [(TPP)TiO]$^-$ generated under the same experimental conditions.[29] Signals corresponding to a titanium(III) porphyrin species were not observed.

Spectroelectrochemistry of (TmTP)Ti(η^2-S_2) was not carried out in detail, but the complex has properties similar to those of both (TPP)Ti(η^2-S_2) and (TpTP)Ti(η^2-S_2) (see earlier sections of this paper). The basicity of the three porphyrin rings are also similar. Thus, these facts and the similar voltammetric data for (TmTP)Ti(η^2-S_2), (TPP)Ti(η^2-S_2), and (TpTP)Ti(η^2-S_2) allow one to describe the first reduction as shown in eq 1, where P = TPP, TpTP, TmTP, or $TpCF_3PP$.

$$(P)Ti(\eta^2\text{-}S_2) + e^- \Leftrightarrow [(P^\bullet)(\eta^2\text{-}S_2)]^- \quad (1)$$

The second reduction of (P)Ti(η^2-S_2) was also monitored by thin-layer spectroelectrochemistry. Only small changes occur in the Soret region of the doubly reduced product as compared to the spectrum of [(P)Ti(η^2-S_2)]$^-$. The two Q bands of the singly reduced species disappear as the reduction proceeds, and these bands are replaced by a single broad band centered at 620 nm. Isosbestic points are present during the first 2 min of electrolysis. In addition, the spectrum of the first reduced species could be regenerated if the potential was reset to −1.15 V during this period. However, the reduction process was not reversible when bulk electrolysis is carried out at −1.40 V for periods longer than 2–3 min and neither molar absorptivities nor wavelength maxima of stable products could be recorded.

Controlled-potential coulometry carried out during the second reduction of ($TpCF_3PP$)Ti(η^2-S_2) gave values of n higher than 2.0, but an n = 1.8 was obtained for (TPP)Ti(η^2-S_2) when the reduction was carried out at a controlled potential of −1.6 V. This latter value is in agreement with a global transfer of two electrons to the initial species. The green solution generated at this potential does not exhibit an ESR signal at low temperature. When the potential was reset to 0.0 V, the solution returned to the initial brown amber color, indicating a reversibility of the second reduction.

On the basis of all of these data, the second electron transfer is assigned as occurring at the porphyrin π ring system to give a porphyrin π dianion. This species is not stable at time scales longer than a few minutes and is quite sensitive to experimental conditions, in particular to the presence of trace water or trace molecular oxygen in solution. However, one can still describe the electrode reaction as occurring via eq 2, where P = TPP, TpTP, or $TpCF_3PP$.

$$[(P^\bullet)Ti(\eta^2\text{-}S_2)]^- + e^- \Leftrightarrow [(P)Ti(\eta^2\text{-}S_2)]^{2-} \quad (2)$$

The time-resolved spectral changes obtained during thin-layer electrolysis of (TpTP)Ti(η^2-Se_2) at −1.2 V are shown in Figure 6b. The spectrum of the singly reduced product is similar to the spectra of singly reduced (TPP)Ti(η^2-S_2), (TpTP)Ti(η^2-S_2), or ($TpCF_3PP$)Ti(η^2-S_2) and indicates that a π anion radical is generated upon the first one-electron addition to the diselenium complex.

The radical anion generated in the reduction of (TpTP)Ti(η^2-Se_2) is not stable, and a spectrum differing from the initial one was observed when the potential was reset to 0.0 V after 1 min of controlled-potential electrolysis at −1.2 V. This new spectrum appears to be that for a mixture of the original compound and some (TpTP)TiO, which has a Soret band at 428 nm. The amount of oxo species generated seemed to vary with experimental conditions and to increase in the presence of trace O_2 or trace water in solution. Controlled-potential coulometry yielded complicated current–time curves and faradaic values much higher than 1. The second reduction of (P)Ti(η^2-Se_2) also gave complicated coulometric measurements and complex spectral data. Thus, the perseleno derivatives seem to be reversibly reduced only on the cyclic voltammetric time scale.

Finally, it has already been pointed out that the titanium–selenium bonds of (P)Ti(η^2-Se_2) are weaker than the titanium–sulfur bonds in (P)Ti(η^2-S_2). This is also evidenced by the higher

(49) The UV–visible peak maxima and ϵ (in parentheses) of singly reduced (TPP)TiO in CH_2Cl_2, 0.1 M TBAP as measured in our laboratory are as follows: 443 nm (6.2×10^4 M^{-1}·cm^{-1}); 678 nm (1.9×10^4 M^{-1}·cm^{-1}, very broad).

reactivity of electrogenerated $[(P)Ti(\eta^2\text{-}Se_2)]^-$ in solution.

Oxidation of $(P)Ti(\eta^2\text{-}S_2)$ and $(P)Ti(\eta^2\text{-}Se_2)$. The first oxidation of $(P)Ti(\eta^2\text{-}S_2)$ and $(P)Ti(\eta^2\text{-}Se_2)$ occurs at E_p values between 0.69 and 1.12 V depending upon the specific porphyrin macrocycle and chalcogen ligand (see Table X). These oxidations are totally irreversible in that there is no return peak. However, the peaks are characterized by an $|E_p - E_{p/2}| = 75 \pm 5$ mV, which suggests that a fast following chemical reaction can account for the irreversibility.

The difference between E_p values for oxidation of $(P)Ti(\eta^2\text{-}S_2)$ and $(P)Ti(\eta^2\text{-}Se_2)$ is 0.18 ± 0.03 V with the perseleno complexes being easier to oxidize. The ratio between peak currents for the first oxidation and the first reduction of $(P)Ti(\eta^2\text{-}Y_2)$ amounts to $\approx$1.6 for $(TpTP)Ti(\eta^2\text{-}S_2)$ and $(OEP)Ti(\eta^2\text{-}S_2)$ and to $\approx$1.2 for $(TpTP)Ti(\eta^2\text{-}Se_2)$ and $(OEP)Ti(\eta^2\text{-}Se_2)$ (see Figure 5). The electrochemical behavior of $(P)Ti(\eta^2\text{-}Y_2)$ differs from that of $(P)Ti(\eta^2\text{-}O_2)$ or (P)TiO in that the latter compounds undergo reversible oxidations. These occur at $E_{1/2} = 1.19$ and 1.20 V for $(TPP)Ti(\eta^2\text{-}O_2)$ and (TPP)TiO in CH_2Cl_2 and at $E_{1/2} = 1.02$ and 1.04 V for $(OEP)Ti(\eta^2\text{-}O_2)$ and (OEP)TiO in the same solvent system, respectively. $(OEP)Ti(\eta^2\text{-}O_2)$ and $(TPP)Ti(\eta^2\text{-}O_2)$ undergo two one-electron ring-centered oxidations yielding first a π cation radical and then a dication.[29] These values can be compared to $E_p = 0.77$ V for the oxidation of $(TPP)Ti(\eta^2\text{-}Se_2)$ or to $E_p = 0.69$ V for the oxidation of $(OEP)Ti(\eta^2\text{-}Se_2)$ in CH_2Cl_2. The E_p values for oxidation of $(P)Ti(\eta^2\text{-}S_2)$ and $(P)Ti(\eta^2\text{-}Se_2)$ thus occur at less positive potentials (relative to the first reduction potentials) than is expected for a ring-centered reaction (see Table X).[47]

The oxidation peak potentials of the perselenio and perthio derivatives may be shifted to less positive potentials because a chemical reaction follows the electron transfer (such as an EC or ECE mechanism)[50] or because the oxidation does not occur at the porphyrin π ring system. A combination of both factors is possible for the present series of compounds. It has already been shown that (TPP)Ti(tdt) (tdt = toluenedithiol) in CH_2Cl_2 undergoes an initial oxidation at the toluenedithiol ligand.[21] $MoO(\eta^2\text{-}S_2)(R_2dtc)_2$ and $WO(\eta^2\text{-}S_2)(R_2dtc)_2$ (R = alkyl, dtc = dithiocarbamate) also undergo initial irreversible oxidations at the side-on perthio ligand, and these reactions occur at around 1.0 V vs Ag/AgCl.[40] Thus, these data, along with the observed dependence of E_p on the specific axial ligand of the investigated complexes, suggest that the side-on chalcogen ligand is directly involved in this oxidation process or that it has a strong influence on the total mechanism. Studies to elucidate the exact oxidation mechanism of $(P)Ti(\eta^2\text{-}S_2)$ and $(P)Ti(\eta^2\text{-}Se_2)$ are now in progress.

(50) Nicholson, R. S.; Shain, I. *Anal. Chem.* **1964**, *36*, 706.

Acknowledgment. The support of the CNRS, the National Science Foundation (Grants CHE-8822881 and INT-8413696), and NATO (Grant 0168/87) is gratefully acknowledged. Professor Claude Lecomte (University of Nancy I, Nancy, France) is gratefully acknowledged for helpful discussions.

Registry No. $(TPP)Ti(\eta^2\text{-}S_2)$, 119890-42-5; $(TmTP)Ti(\eta^2\text{-}S_2)$, 119890-43-6; $(TpTP)Ti(\eta^2\text{-}S_2)$, 119890-53-8; $(TpCF_3PP)Ti(\eta^2\text{-}S_2)$, 119890-56-1; $(TMP)Ti(\eta^2\text{-}S_2)$, 119890-45-8; $(OEP)Ti(\eta^2\text{-}S_2)$, 119890-46-9; $(TPP)Ti(\eta^2\text{-}Se_2)$, 119890-47-0; $(TmTP)Ti(\eta^2\text{-}Se_2)$, 119890-48-1; $(TpTP)Ti(\eta^2\text{-}Se_2)$, 119890-49-2; $(TpCF_3PP)Ti(\eta^2\text{-}Se_2)$, 119890-50-5; $(TMP)Ti(\eta^2\text{-}Se_2)$, 119890-51-6; $(OEP)Ti(\eta^2\text{-}Se_2)$, 119890-52-7; Cp_2TiS_5, 12116-82-4; Cp_2TiSe_5, 12307-22-1; (TPP)TiF, 71454-15-4; (TmTP)TiF, 119890-38-9; (TpTP)TiF, 119890-39-0; (TMP)TiF, 119890-41-4; $(TpCF_3PP)TiF$, 119890-40-3; (OEP)TiF, 71414-23-8; $(TPP)TiF_2$, 66350-84-3; $(TpTP)TiF_2$, 119890-34-5; $(TmTP)TiF_2$, 119890-33-4; $(TMP)TiF_2$, 119890-36-7; $(TpCF_3PP)TiF_2$, 119890-35-6; $(OEP)TiF_2$, 119890-37-8.

Supplementary Material Available: Tables of positional parameters of hydrogen atoms, general displacement parameter expressions (U's), bond distances and angles, least-squares planes, and experimental crystallographic conditions (9 pages); a table of observed and calculated structure factors for $(TpTP)Ti(\eta^2\text{-}S_2)$ (16 pages). Ordering information is given on any current masthead page.